Synthesis and theoretical investigation of phenanthrodithiophene diimide

Yen-Ting Chen,[a‡] **Yen-Yu Chen,**[c‡] **Yu-Ying Lai,**[c*] **and Yen-Ju Cheng**[ab*]

[a]Department of Applied Chemistry, National Yang Ming Chiao Tung University, 1001 University Road, Hsin-Chu 30010, Taiwan
[b]Center for Emergent Functional Matter Science, National Yang Ming Chiao Tung University, 1001 University Road, Hsinchu, 30010, Taiwan
[c]Institute of Polymer Science and Engineering, National Taiwan University, Taipei 106319, Taiwan
[‡]Yen-Ting Chen and Yen-Yu Chen contribute equally
Email: yjcheng@nycu.edu.tw and yuyinglai@ntu.edu.tw

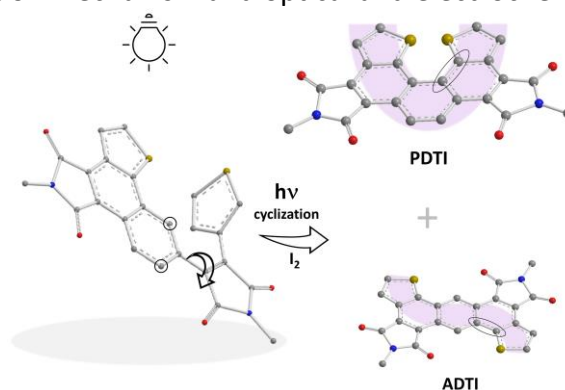**Dedicated to Prof. Tien-Yau Luh on the occasion of his 76th anniversary**

Abstract

Construction of a phenanthrodithiophene diimide core has been accomplished through photo-induced 6π electrocyclization. It is generated with the formation of anthradithiophene diimide. The product distribution is illuminated by the help of DFT calculations. The discrepancy in the optical and electrochemical properties between both compounds is identified. Time-dependent DFT calculations are carried out, yielding theoretical UV-vis spectra, which agree well with the experimental patterns. Electronic transitions for the two compounds can be clarified. Overall, this study provides a new synthetic approach to accessing phenanthrodithiophene diimide and elucidates the reaction mechanism and optical and electrochemical properties.

Page 1 of 16

Introduction

Fields related to organic semiconductors, such as organic photovoltaics,[1-4] organic field-effect transistors,[5-8] and organic light-emitting diodes,[9-12] have been benefited appreciably from the expansion of materials library, in which the structural diversity plays a vital role. Numerous chemical functionalities have been employed in developing building blocks for organic semiconductors. Among them, imide shows great promise. A couple of imide-based structures are included in Scheme 1. Naphthalene diimide (**NDI**) is a classical imide-based building block and often functions as an electron-deficient group in synthesizing donor-acceptor copolymers.[13-16] Abundant studies derived from **NDI** can be found in the literature.[17-26] Fused arenes have been recognized to be effective in regulating π-extension and corresponding stacking.[27-37] Outwardly fusing **NDI** with two thiophenes gives naphthodithiophene diimide (**NDTI**). A key synthetic step involves addition of the sulfide anion to the ethyne group and oxidative dehydrogenation to yield the **NDTI** core.[38, 39] Anthradithiophene substituting for naphthodithiophene furnishes anthradithiophene diimide (**ADTI**). Palladium-catalyzed direct arylation has been applied to generate the **ADTI** core.[40] Great potential of **NDTI** and **ADTI** in organic electronics has been demonstrated.[41-48]

Phenanthrodithiophene diimide (**PDTI**) has a distinctive curved aromatic frame. The materials properties could be diversified by taking advantage of the isomeric structure. In this study, a synthetic route to **PDTI** is established. The ultimate synthetic step to **PDTI** is accompanied with the formation of **ADTI**, which is clarified by the help of DFT calculations. **PDTI** is compared with **ADTI** and their optical and electrochemical properties are discussed. In the synthesis, photo-induced 6π electrocyclization plays a crucial role, and the formation mechanism is proposed.


NDI   **NDTI**   **ADTI**   **PDTI**
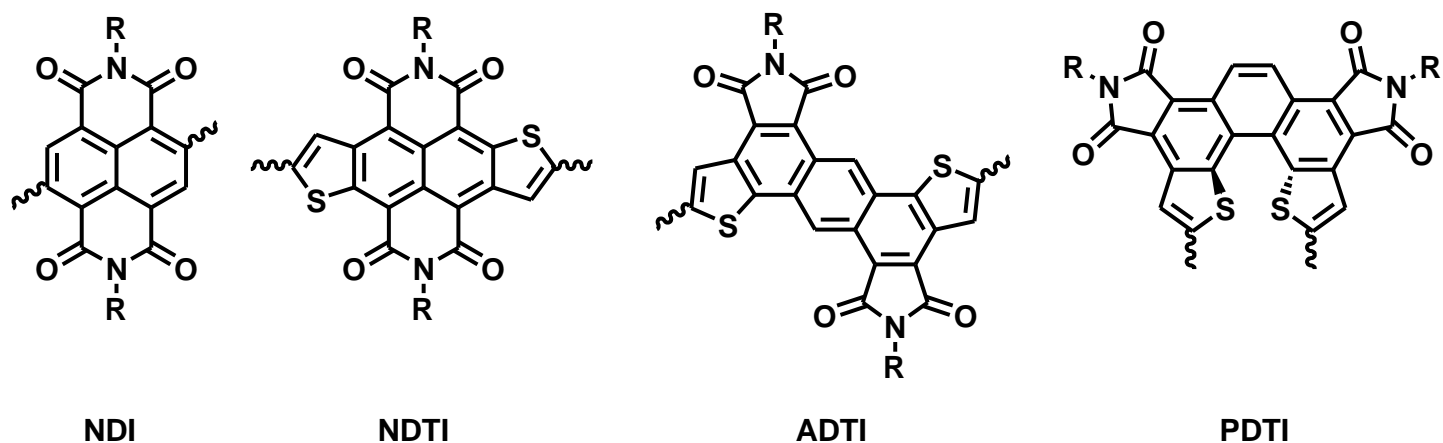
Scheme 1. Imide-based structures.

Results and Discussion

ADTI. Synthesis of **ADTI** and **PDTI** is summarized in Scheme 2. *N*-(2-hexyldecyl)phthalimide (**1**) was attained by nucleophilic substitution of bromide in 2-hexyldecyl bromide by potassium phthalimide. Treatment of **1** with hydrazine in methanol yielded 2-hexyldecyl amine (**2**), which then reacted with 2,3-dibromomaleic anhydride (**3**) derived from bromination of maleic anhydride to afford 2,3-dibromo-*N*-hexyldecyl maleimide (**4**). Compound **5** was generated by Suzuki–Miyaura coupling of **4** with thiophene-3-boronic acid pinacol ester at

room temperature. It has to noted that an elevated temperature encouraged further coupling between **5** and thiophene-3-boronic acid pinacol ester. Suzuki–Miyaura coupling was performed again to furnish compound **6**, which was illuminated by a medium-pressure mercury lamp in the presence of iodine, resulting in **ADTI** and **PDTI** in 16% and 30% yield, respectively. In principle, **ADTI** would exhibit four ^1H–^{13}C heteronuclear multiple bond correlations (HMBCs) for H_1 whereas three correlations would be present for **PDTI**, which is consistent with the results given by HMBC spectroscopy (Figure 1).
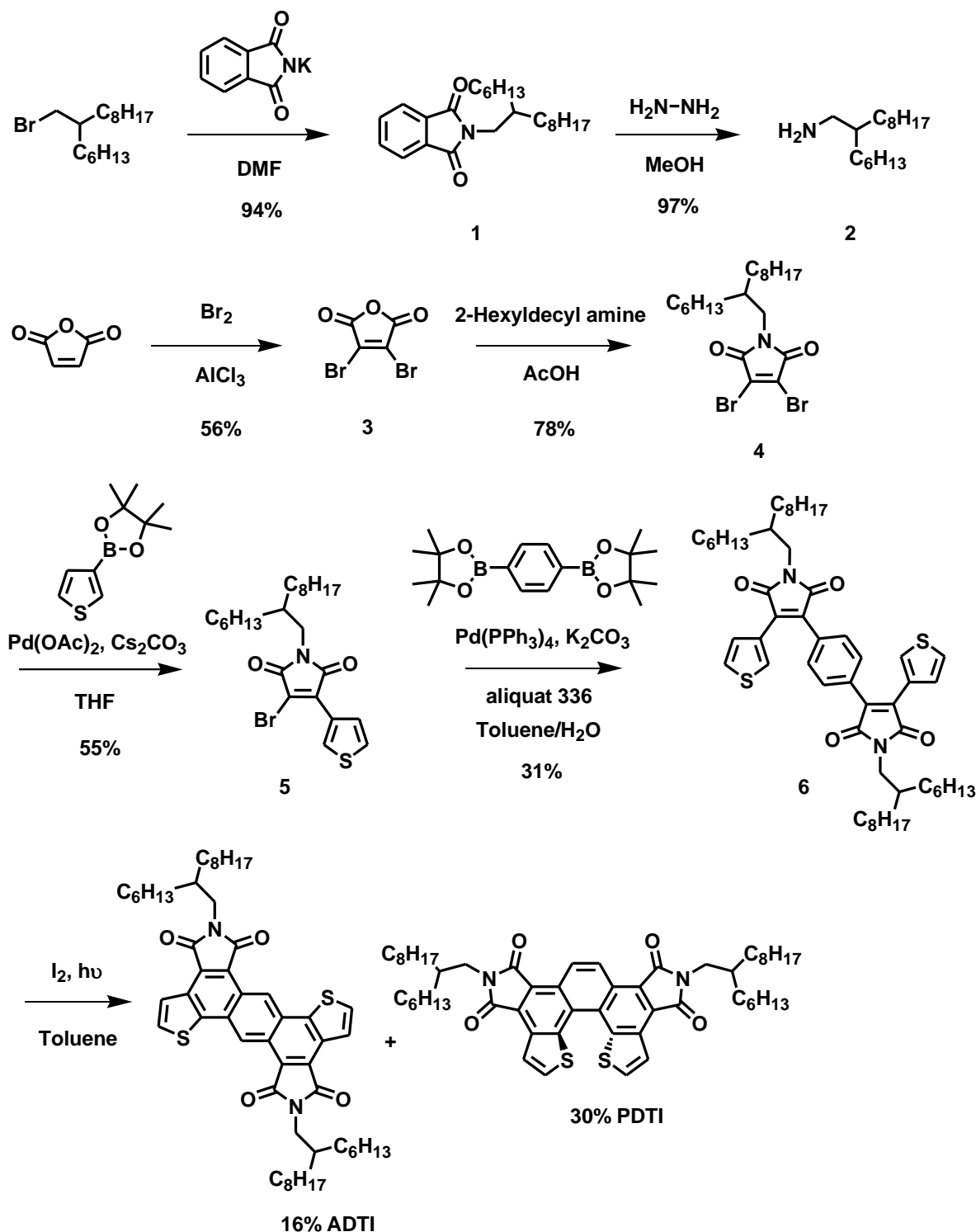
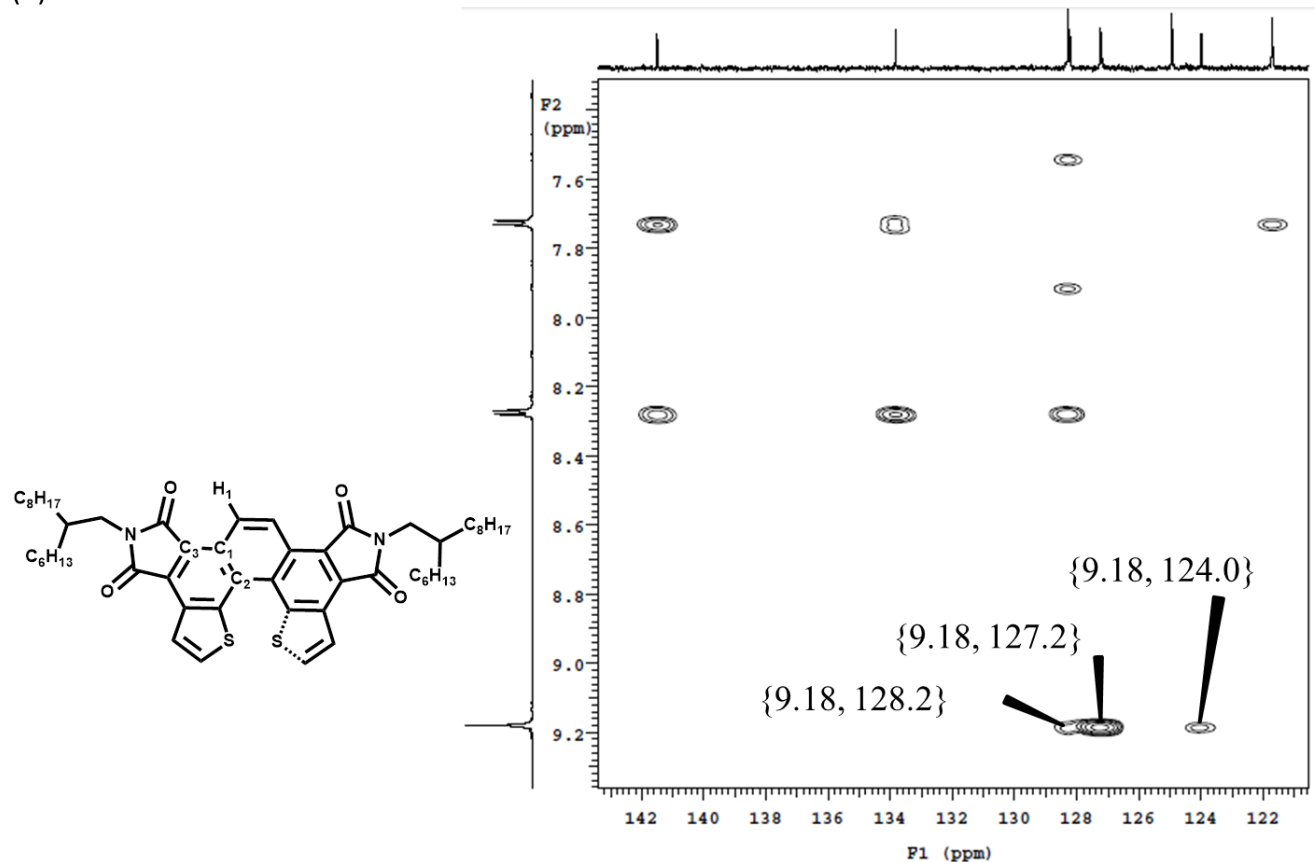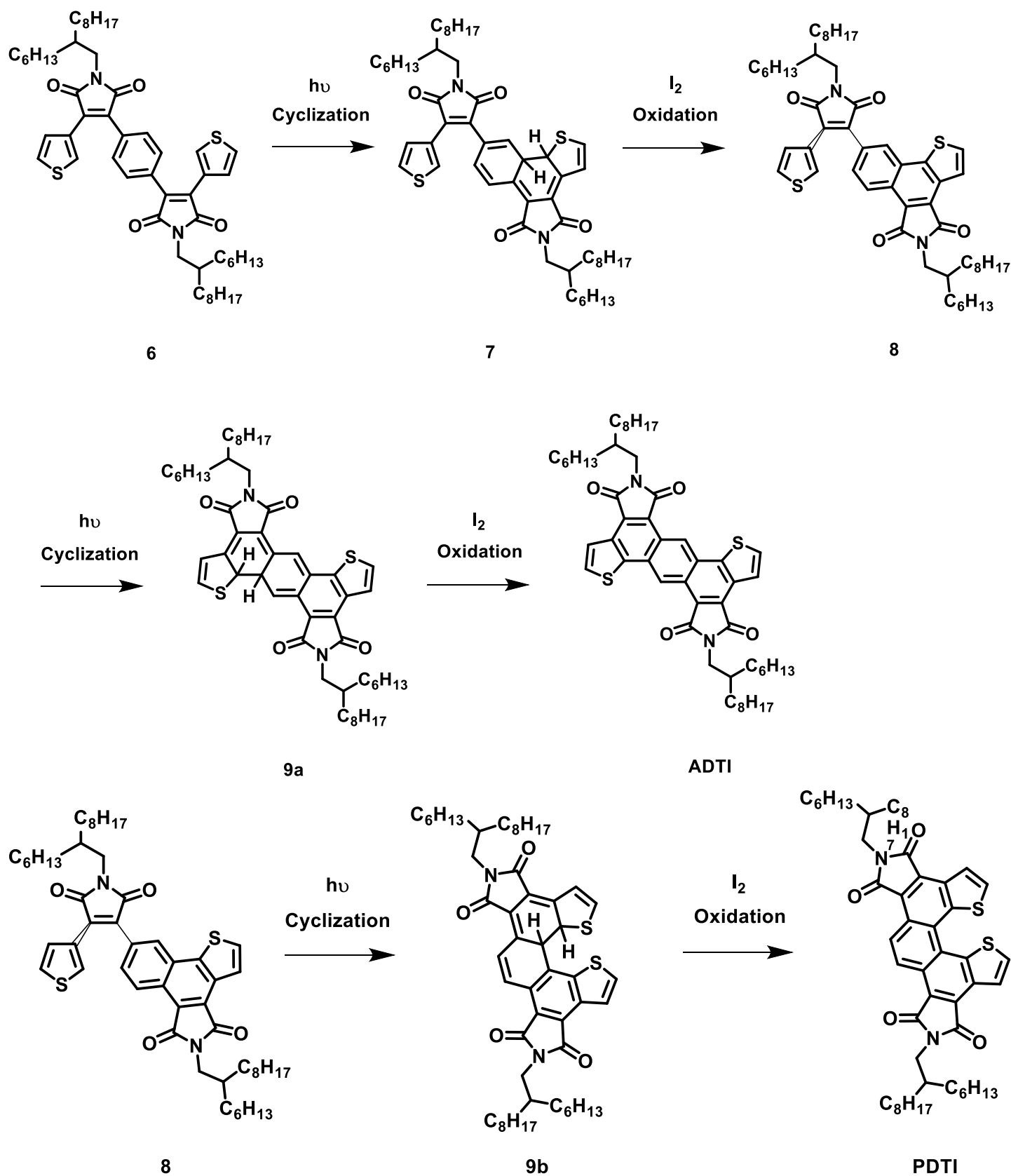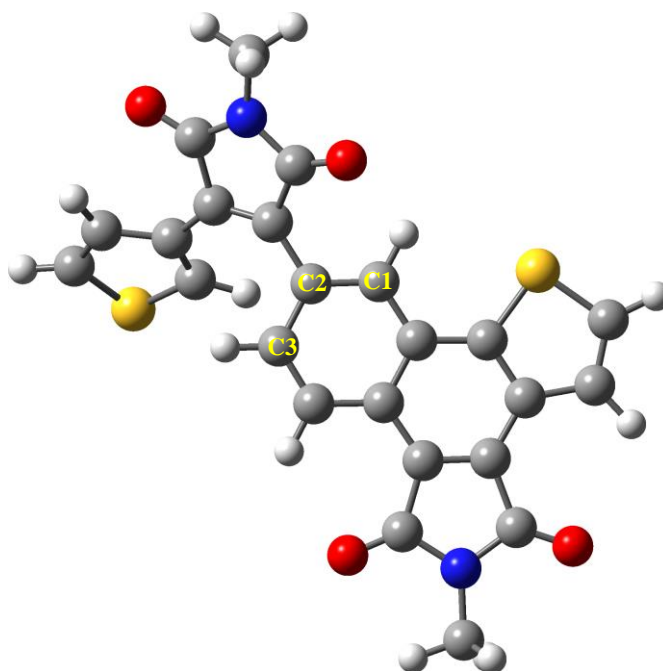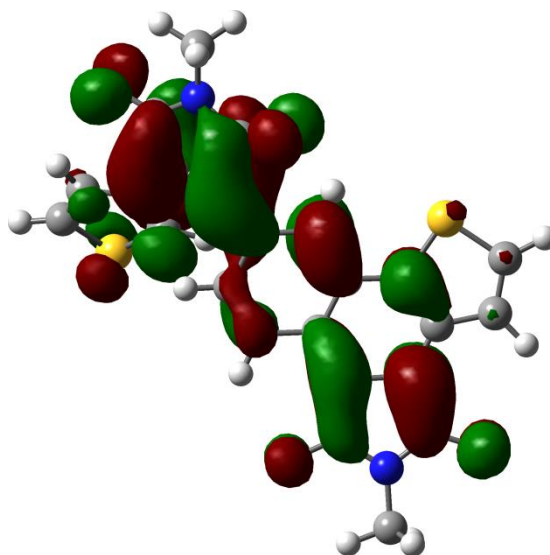**Scheme 2**. Synthesis of **ADTI** and **PDTI**.

(a)
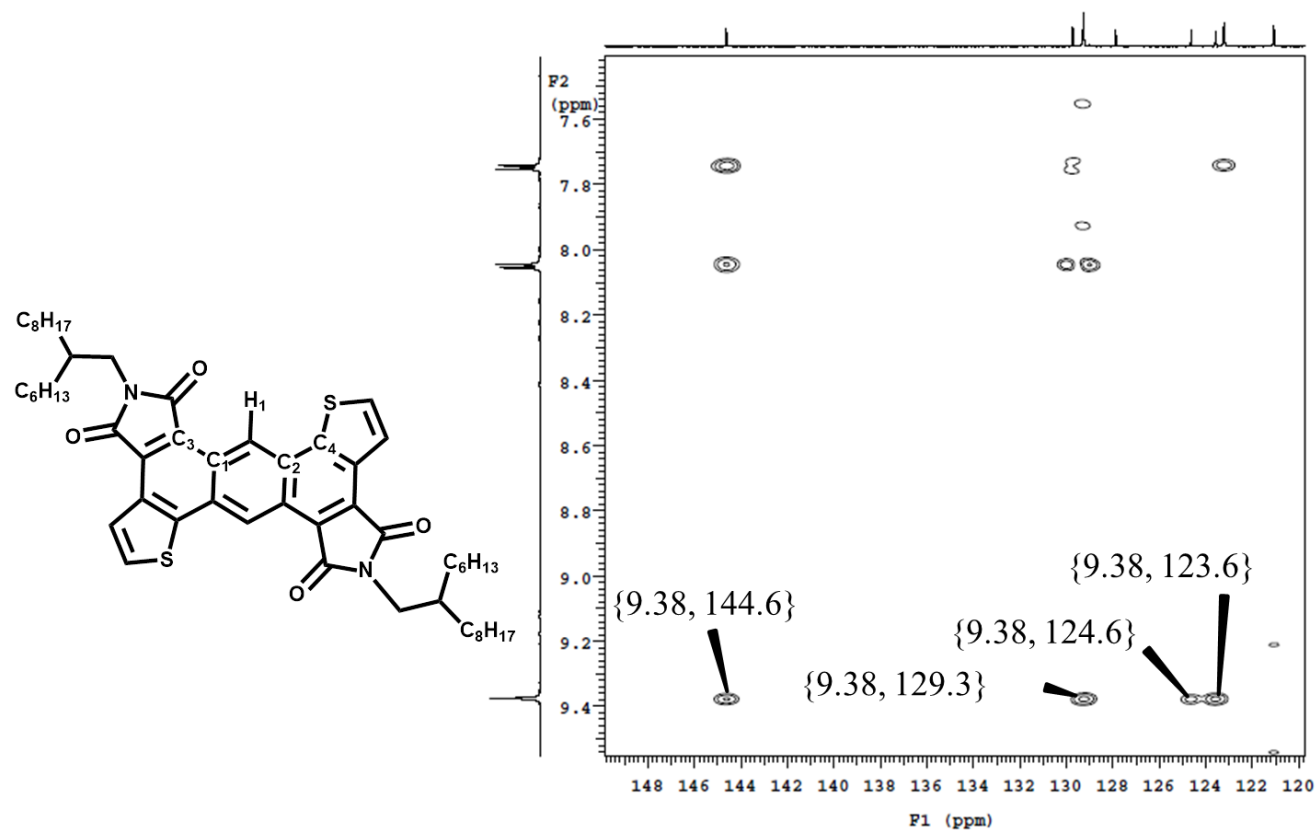
(b)

Figure 1. HMBC spectra of (a) **ADTI** and (b) **PDTI**.

Scheme 3. Proposed mechanism for the formation of **ADTI** and **PDTI**.

(a) Optimized Structure of **8**[a]

Bond length: C1–C2: 1.38 Å, C2–C3: 1.42 Å   Bond order: C1–C2: 1.48, C2–C3: 1.25

(b) LUMO of **8**

Atomic orbital contribution in LUMO[a]: C1: 4.672853%, C2: 4.452770%, C3: 1.083244%

Figure 2. (a) Optimized Structure and (b) LUMO contour (isovalue = 0.02 au) of **8** calculated at the CAM-B3LYP/6-311G(d,p) level of theory.
[a] 2-Hexyldecyl is replaced by methyl and Wiberg bond order was calculated by Natural Bond Orbital 5.9.

A proposed mechanism is depicted in Scheme 3, in which compound **6** goes through intramolecular 6π electrocyclization and oxidation twice to produce **ADTI** and **PDTI**. DFT calculations were performed in order to

gain an insight into the regioselectivity for this photo-induced cyclization. Gibbs free energy at the CAM-B3LYP/6-311G(d,p) level of theory indicates that **ADTI** is thermodynamically more stable than **PDTI** by 11.6 kcal mol^{-1}, being inconsistent with the experimental yield (16% versus 30%). As shown in Scheme 3, the different regioisomeric products formed are related to the intramolecular 6π electrocyclization of **8**. Optimized structure of **8** in Figure 2 reveals that C1–C2 has stronger double-bond character than C2–C3 in terms of bond length and bond order. On the basis of Woodward-Hoffmann rules, LUMO of **8** is the functional orbital for photo-stimulated electrocyclization. Atomic orbital composition of LUMO in **8** was obtained by Hirshfeld method implemented in MULTIWFN 3.3.8,[49] estimating that C1 has greater atomic-orbital contribution than C3 (Figure 2). In other words, the electron-density of C1 is higher than that of C3 in the LUMO. Atomic orbital analysis in conjunction with the calculated bond length and bond order suggests that C1–C2 might exhibit superior reactivity to C2–C3 in the photo-induced 6π electrocyclization, accounting for the experimental regioselectivity.

Optimized structures of **ADTI** and **PDTI** are described in Figure 3. A planar conjugated framework is observed for **ADTI** whereas **PDTI** shows a twisted plane with two isomeric structures. The inversion barrier between the two enantiomers for **PDTI** is calculated to be 10.90 kcal mol^{-1}, which should be overcame readily at room temperature. UV-vis absorption of **ADTI** and **PDTI** is illustrated in Figure 4. Different absorption pattern is perceived between the two constitutional isomers and the E_g^{opt} of **ADTI** is smaller than that of **PDTI** (Table 1), which is associated with the distorted conjugated structure of **PDTI**.

(a) Optimized Structure of **ADTI**
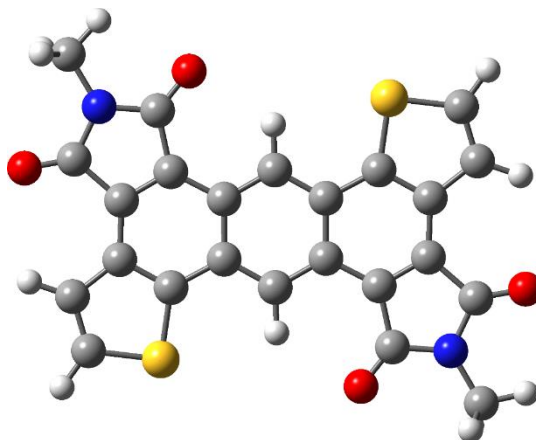
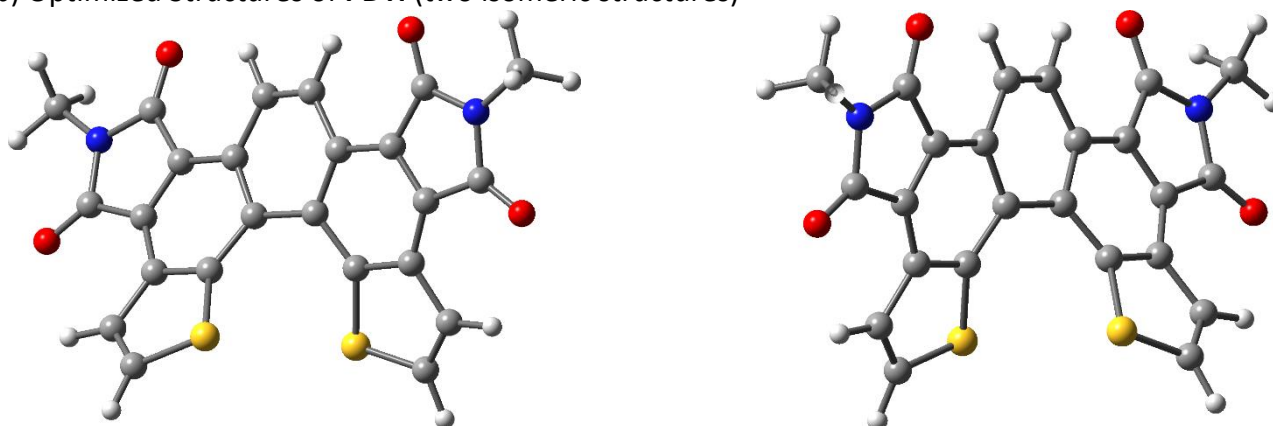(b) Optimized Structures of **PDTI** (two isomeric structures)

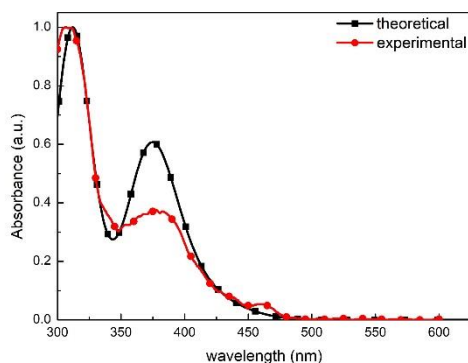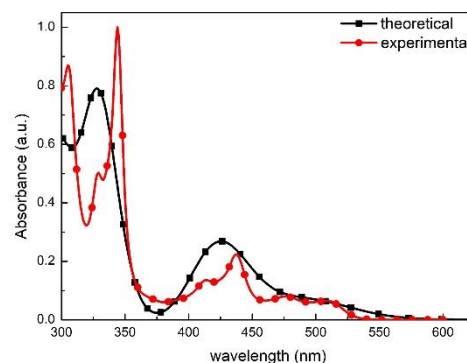**Figure 3.** Optimized structures of (a) **ADTI** and (b) **PDTI**.

PDTI

ADTI

Figure 4. Experimental and theoretical[a] UV-vis absorption spectra of **PDTI** and **ADTI**.
[a]Level of theory: TD-MPW1PW91/6-311G(d,p)/PCM=CH_2Cl_2//CAM-B3LYP/6-311G(d,p)

Table 1. Optical and electrochemical properties of **PDTI** and **ADTI**

	HOMO[a] (eV)	LUMO[b] (eV)	E_g^{ele} [c] (eV)	E_g^{opt} [d] (eV)
PDTI	−5.96	−3.25	2.71	2.57
ADTI	−5.92	−3.45	2.47	2.32

[a]Highest occupied molecular orbital. [b]Lowest unoccupied molecular orbital. [c]Electrochemical energy gap. [d]Optical energy gap determined by the onset of absorption.

Time-dependent density-functional theory (TD-DFT) calculations were performed for **PDTI** and **ADTI**. The experimental and theoretical UV-vis spectra correlate well to each other (Figure 4). Calculated HOMO/LUMO energy, absorption maximum, oscillator strength, and configuration of the excited states are summarized in Table 2. Contours of HOMOs and LUMOs are illustrated in Figure 5. Interpretation of electronic transitions for **PDTI** and **ADTI** can thus be achieved.

Table 2. Calculated HOMO/LUMO energy, excitation energy, oscillator strength, and configurations (with large CI coefficients) of the excited states[a]

|	HOMO (eV)	LUMO (eV)	$\lambda_{max,exp}$[b] (nm)	λ_{cal}[c] (nm)	oscillator strength	Configuration[d]
PDTI	−6.56	−2.90	462	428	0.0259	H→L
				398	0.0579	H−1→L
			378	374	0.2973	H→L+1
				370	0.0314	H−2→L
				349	0.0497	H−1→L+1
				324	0.0361	H→L+2
			307	314	0.3934	H−2→L+1
ADTI	−6.35	−3.16	510	495	0.0514	H→L
			476			
			437	425	0.2125	H−1→L
			413			
			344	329	0.6037	H→L+2
			329			
			305	299	0.3831	H−1→L+2

[a]TD-MPW1PW91/6-311G(d,p)/PCM=CH_2Cl_2//CAM-B3LYP/6-311G(d,p); Aliphatic moieties are simplified by the methyl group. [b]Experimental absorption maximum. [c]Calculated absorption maximum. [d]Configurations with largest coefficients in the CI expansion of each state are listed.

PDTI
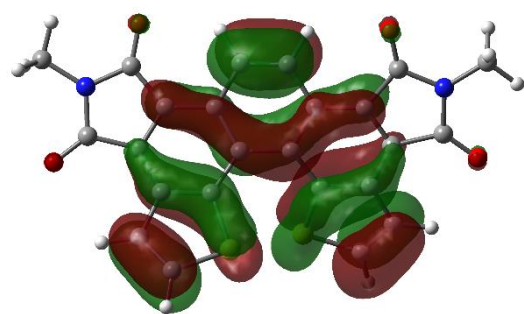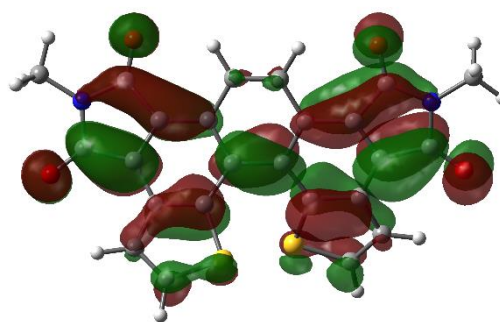
HOMO   LUMO

ADTI
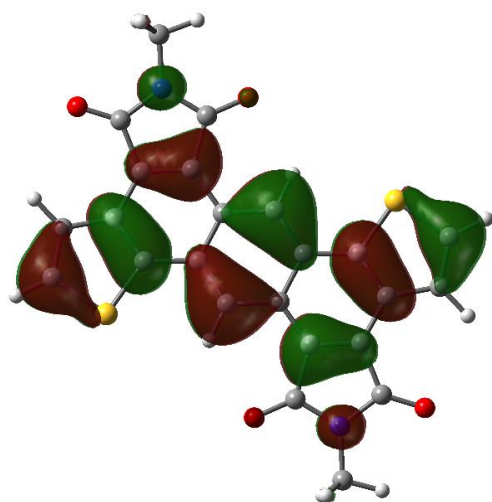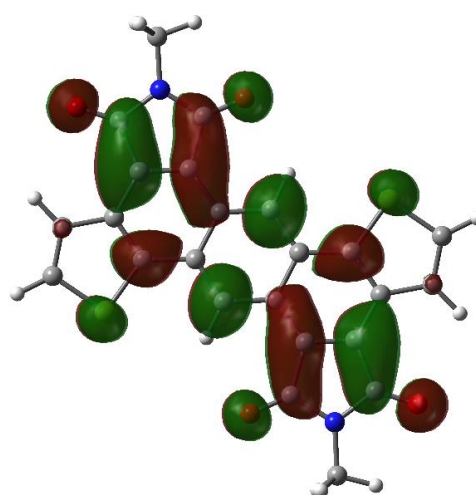
HOMO   LUMO

Figure 5. Plots (isovalue = 0.02 au) of HOMOs and LUMOs.

Conclusions

Construction of the **PDTI** core has been accomplished. Photo-induced 6π electrocyclization is a key step for synthesis of **PDTI**. Formation of **PDTI** is accompanied with that of **ADTI**. The product distribution can be elucidated by the help of DFT calculations. **PDTI** is compared with **ADTI**. The disparity in the optical and electrochemical properties between the isomers is identified. TD-DFT is performed and good agreement is recognized between the experimental and theoretical UV-vis spectra, providing better understanding into electronic transitions for **PDTI** and **ADTI**. Overall, this study provides a new synthetic approach to accessing **PDTI** and elucidates the reaction mechanism and optical and electrochemical properties.

Experimental Section

General. NMR measurements are reported for a Bruker-400 MHz spectrometer. Chemical shifts (δ values) are reported in ppm with respect to Me$_4$Si (δ = 0 ppm) for ^{13}C and ^{1}H NMR. Coupling constants (J) are given in Hz. ^{13}C NMR was proton broad-band-decoupled. Multiplicities of peaks are denoted by the following abbreviations: s, singlet; d, doublet; t, triplet; m, multiplet; br, broad; dd, doublet of doublets. Heteronuclear multiple bond correlation spectroscopy (HMBC) was performed on a Varian 500 MHZ spectrometer. UV-Vis spectra were collected on a Hitachi U-4100 spectrometer. Mass spectra were collected by the Instrumentation Center, National Chiao Tung University. Electrochemical cyclic voltammetry (CV) was conducted on CH Instruments CHI661D. Platinum wire was the counter electrode. Glassy carbon and Ag/AgCl electrode were used as the working electrode and the reference electrode, respectively, while 0.1 M tetrabutylammonium hexafluorophosphate in CH$_2$Cl$_2$/CH$_3$CN was the electrolyte. The scan rate was 100 mV/S. CV curves were calibrated using ferrocence as the standard, whose oxidation potential is set at –4.8 eV with respect to zero vacuum level. The HOMO energy levels were obtained from the equation HOMO = –(E$_{ox}^{onset}$ – E$_{(ferrocene)}^{onset}$ + 4.8) eV. The LUMO levels were obtained from the equation LUMO = –(E$_{red}^{onset}$ – E$_{(ferrocene)}^{onset}$ + 4.8) eV.

Synthesis of 1. A DMF solution (20 mL) of 2-hexyldecyl bromide (5 g, 0.0164 mol) and phthalimide potassium salt (3.22 g, 0.0173 mol) was stirred at 90 °C for 16 h. The mixture was cooled to room temperature, poured into water (100 mL) and extracted with dichloromethane (50 mL×2). The organic fraction was dried over anhydrous MgSO$_4$, filtered, and concentrated under vacuum. The crude mixture was purified by column chromatography to furnish *N*-(2-hexyldecyl)phthalimide as a colorless oil (5.75 g, 94% yield): ^{1}H NMR (400 MHz, CDCl$_3$) δ 7.85–7.82 (m, 2H), 7.73–7.69 (m, 2H), 3.57 (d, J = 8 Hz, 2H), 1.90–1.85 (m, 1H), 1.29–1.24 (m, 24H), 0.88–0.84 (m, 6H).

Synthesis of 2. A mixture of *N*-(2-hexyldecyl)phthalimide (3.9 g, 0.0105 mol), hydrazine monohydrate (80%, 1.9 mL, 0.0315 mol), and methanol (50 mL) was stirred at 95 °C for 16 h. The mixture was cooled to room temperature, concentrated under vacuum, poured into KOH$_{(aq)}$ (10%, 100 mL), and extracted with dichloromethane (50 mL×2). The collected organic layer was washed with brine (100 mL×2), dried over anhydrous MgSO$_4$, filtered, and concentrated under reduced pressure. After removal of solvent, 2-hexyldecyl amine was furnished as a colorless oil (2.47 g, 97% yield): ^{1}H NMR (400 MHz, CDCl$_3$) δ 2.60 (d, J = 4.0 Hz, 2H), 1.32–1.27 (m, 25H), 0.88 (t, J = 8.0 Hz, 6H).

Synthesis of 3. Maleic anhydride (1.5 g, 0.0153 mol), aluminum chloride (28 mg, 0.2 mmol), bromine (4.9 g, 0.03 mol) were put in a sealed tube. The mixture was heated with stirring at 120 °C for 18 h, cooled to room temperature, diluted with ethyl acetate (15 mL), washed with saturated Na$_2$S$_2$O$_{3(aq)}$ (50 mL), and extracted with dichloromethane (50 mL×2). The collected organic layer was washed with brine (100 mL×2), dried over anhydrous MgSO$_4$, filtrated, and concentrated under vacuum. After the removal of the solvent, the product was obtained as a white powder (2.0 g, 51% yield). ^{13}C NMR (100 MHz, CDCl$_3$) δ 158.5, 131.3.

Synthesis of 4. A mixture of 2,3-dibromomaleic anhydride (2.1g, 0.008 mol), 2-hexyldecyl amine (2g, 0.008 mol), and acetic acid (20 mL) was stirred at refluxing temperature for 16 h. The mixture was cooled to room temperature, poured into water (100 mL) and extracted with dichloromethane (50 mL×3). The organic layer was washed with water (100 mL×2), dried over anhydrous MgSO$_4$, filtered, and concentrated under vacuum. The crude mixture was purified by column chromatography (hexane:ethyl acetate = 20:1). After removal of solvent, the product was afforded as a yellow oil (3.1 g, 78% yield): ^{1}H NMR (400 MHz, CDCl$_3$) δ 3.49 (d, J = 7.1 Hz, 2H), 1.79–1.65 (m, 1H), 1.36–1.11 (m, 24H), 0.88 (t, J = 6.8 Hz, 6H). ^{13}C NMR (100 MHz, CDCl$_3$) δ 164.2, 129.2, 43.9, 37.0, 31.9, 31.7, 31.3, 29.8, 29.5, 29.5, 29.2, 26.2, 26.1, 22.6, 22.6, 14.1, 14.0.

Synthesis of 5. A THF solution (40 mL) of 2,3-dibromo-*N*-hexyldecylmaleimide (1 g, 0.002 mol), thiophene-3-boronic acid pinacol ester (484 mg, 0.002 mol), Cs_2CO_3 (1.54g, 0.004 mol), and $Pd(OAc)_2$ (23mg, 0.1 mmol) was stirred at room temperature for 16 h. The mixture was poured into brine (50 mL), extracted with ethyl acetate (50 mL×2), dried over anhydrous $MgSO_4$, filtered, and concentrated under vacuum. The residue was purified by column chromatography (hexane:ethyl acetate = 50:1). After removal of solvent, the product was obtained as a yellow oil (574 mg, 56% yield): ^1H NMR (400 MHz, $CDCl_3$) δ 8.56 (d, *J* = 4 Hz, 1H), 8.07 (d, *J* = 4 Hz, 1H), 7.45 (dd, *J* = 4 Hz, *J* = 4 Hz, 1H), 3.50 (d, *J* = 7.1 Hz, 2H), 1.80 (m, 1H), 1.43–1.20 (m, 24H), 0.89–0.85 (m, 6H). HRMS (EI, M$^+$, $C_{24}H_{36}BrNO_2S$): calcd, 483.1647; found, 483.1652.

Synthesis of 6. A mixture of compound **5** (550 mg, 0.001 mol), 1,4-benzenediboronic acid bis (pinacol) ester (179 mg, 0.5 mmol), K_2CO_3 (315 mg, 0.002 mol), $Pd(PPh_3)_4$ (31mg, 0.026 mmol), aliquat 336, toluene (40 mL), and H_2O (30 mL) was stirred at 95 ºC for 16 h. The mixture was poured into brine (50 mL), extracted with ethyl acetate (50 mL×2), dried over anhydrous $MgSO_4$, filtered, and concentrated under vacuum. The residual mixture was purified by column chromatography (Hexane: Ethyl acetate = 20: 1) to furnish compound **6** as a yellow powder (150 mg, 31% yield). ^1H NMR (400 MHz, CD_2Cl_2) δ 8.10 (dd, *J* = 3.0, 1.3 Hz, 2H), 7.56 (s, 4H), 7.29 (dd, *J* = 5.1, 3.0 Hz, 2H), 7.13 (dd, *J* = 5.1, 1.3 Hz, 2H), 3.50 (d, *J* = 7.2 Hz, 4H), 1.84–1.81 (m, 2H), 1.42–1.27 (m, 48H), 0.86–0.83 (m, 12H). ^{13}C NMR (100 MHz, $CDCl_3$) δ 171.1, 170.9, 132.4, 131.4, 130.6, 130.5, 129.9, 129.0, 127.3, 125.9, 42.7, 37.0, 31.9, 31.8, 31.5, 29.9, 29.6, 29.5, 29.3, 26.31, 26.28, 22.64, 22.62, 14.1. HRMS (FAB, $C_{54}H_{76}N_2O_4S_2$): calcd, 880.5247; found, 880.5247.

Synthesis of ADTI and PDTI. A toluene solution (30 mL) of compound **6** (100 mg, 0.11 mmol) and iodine (144 mg, 0.55 mmol) was illuminated by a medium-pressure mercury lamp for 4 h. The mixture was poured into saturated $Na_2S_2O_{3(aq)}$ (50 mL), extracted with dichloromethane (50 mL×2), dried over anhydrous $MgSO_4$, filtered, and concentrated under vacuum. The mixture was purified by column chromatography (hexane: dichloromethane = 5 : 1). After removal of solvent, **ADTI** and **PDTI** as a mixture (7a : 7b = 1 : 2) were afforded (50 mg, 50% yield). **ADTI** and **PDTI** were further recrystallized with hexane.

ADTI. ^1H NMR (500 MHz, $CDCl_3$) δ 9.37 (s, 2H), 8.05 (d, *J* = 5.2 Hz, 2H), 7.75 (d, *J* = 5.2 Hz, 2H), 3.64 (d, *J* = 7.0 Hz, 4H), 1.95 (m, 2H), 1.43–1.25 (m, 48H), 0.86–0.81 (m, 12H). ^{13}C NMR of **ADTI** (125 MHz, $CDCl_3$) δ 169.8, 168.7, 144.6, 129.7, 129.3, 129.2, 127.9, 124.6, 123.6, 123.2, 121.1, 42.4, 37.4, 31.88, 31.86, 31.61, 31.59, 30.0, 29.7, 29.6, 29.3, 26.5, 26.4, 22.6, 14.1. HRMS (FAB, $C_{54}H_{72}N_2O_4S_2$): calcd, 876.4934; found, 876.4926.

PDTI. ^1H NMR (500 MHz, $CDCl_3$) δ 9.17 (s, 2H), 8.27 (d, *J* = 5.5 Hz, 2H), 7.72 (d, *J* = 5.5 Hz, 2H), 3.70 (d, *J* = 7.5 Hz, 4H), 1.98 (m, 2H), 1.41–1.33 (m, 48H), 0.85–0.83 (m, 12H). ^{13}C NMR of **PDTI** (125 MHz, $CDCl_3$) δ 169.9, 168.9, 144.5, 133.8, 128.3, 128.2, 127.3, 127.2, 124.9, 124.0, 121.7, 42.5, 37.4, 31.9, 31.8, 31.61, 31.59, 30.0, 29.6, 29.5, 29.3, 26.38, 26.37, 22.6, 14.07, 14.06. HRMS (FAB, $C_{54}H_{72}N_2O_4S_2$): calcd, 876.4934; found, 876.4929.

Acknowledgements

Supplementary Material

Computational details, Cartesian coordinates (Å) of the optimized structures, and NMR spectra

References

1. He, C.; Bi, Z.; Chen, Z.; Guo, J.; Xia, X.; Lu, X.; Min, J.; Zhu, H.; Ma, W.; Zuo, L. *Adv. Funct. Mater.* **2022**, *32*, 2112511.
   https://doi.org/10.1002/adfm.202112511
2. Wen, T.J.; Liu, Z.X.; Chen, Z.; Zhou, J.D.; Shen, Z.Q.; Xiao, Y.Q.; Lu, X.H.; Xie, Z.Q.; Zhu, H.M.; Li, C.Z.; Chen, H.Z. *Angew. Chem.* **2021**, *60*, 12964-12970.
   https://doi.org/10.1002/anie.202101867
3. Xie, L.; Song, W.; Ge, J.; Tang, B.; Zhang, X.; Wu, T.; Ge, Z. *Nano Energy* **2021**, *82*, 105770.
   https://doi.org/10.1016/j.nanoen.2021.105770
4. Xu, C.Y.; Chen, H.Y.; Zhao, Z.J.; Gao, J.H.; Ma, X.L.; Lu, S.R.; Zhang, X.L.; Xiao, Z.Y.; Zhang, F.J. *J Energy Chem* **2021**, *57*, 610-617.
   https://doi.org/10.1016/j.jechem.2020.09.025
5. Chen, H.L.; Zhang, W.N.; Li, M.L.; He, G.; Guo, X.F. *Chem. Rev.* **2020**, *120*, 2879-2949.
   https://doi.org/10.1021/acs.chemrev.9b00532
6. Liu, K.; Ouyang, B.; Guo, X.; Guo, Y.; Liu, Y. *Npj Flex Electron* **2022**, *6*, 1.
   https://doi.org/10.1038/s41528-022-00133-3
7. Matsui, H.; Takeda, Y.; Tokito, S. *Org. Electron.* **2019**, *75*, 105432.
   https://doi.org/10.1016/j.orgel.2019.105432
8. Yuvaraja, S.; Nawaz, A.; Liu, Q.; Dubal, D.; Surya, S.G.; Salama, K.N.; Sonar, P. *Chem. Soc. Rev.* **2020**, *49*, 3423-3460.
   https://doi.org/10.1039/c9cs00811j
9. Chen, J.; Liu, H.; Guo, J.; Wang, J.; Qiu, N.; Xiao, S.; Chi, J.; Yang, D.; Ma, D.; Zhao, Z. *Angew. Chem.* **2022**, *134*, e202116810.
   https://doi.org/10.1002/anie.202116810
10. Jeon, S.O.; Lee, K.H.; Kim, J.S.; Ihn, S.G.; Chung, Y.S.; Kim, J.W.; Lee, H.; Kim, S.; Choi, H.; Lee, J.Y. *Nat Photonics* **2021**, *15*, 208-215.
    https://doi.org/10.1038/s41566-021-00763-5
11. Park, I.S.; Yang, M.; Shibata, H.; Amanokura, N.; Yasuda, T. *Adv. Mater.* **2022**, *34*, 2107951.
    https://doi.org/10.1002/adma.202107951
12. Xu, Y.W.; Xu, P.; Hu, D.H.; Ma, Y.G. *Chem. Soc. Rev.* **2021**, *50*, 1030-1069.
    https://doi.org/10.1039/d0cs00391c
13. Barman, S.; Bandyopadhyay, S.; Ghosh, A.; Das, S.; Mondal, T.; Datta, A.; Ghosh, S.; Datta, A. *Chem. Commun.* **2022**, *58*, 10508-10511.
    https://doi.org/10.1039/d2cc02506j
14. Chakraborty, S.; Barman, R.; Ghosh, S. *J. Mater. Chem. B.* **2020**, *8*, 2909-2917.
    https://doi.org/10.1039/c9tb02772f

15. Drewniak, A.; Tomczyk, M.D.; Hanusek, L.; Mielanczyk, A.; Walczak, K.; Nitschke, P.; Hajduk, B.; Ledwon, P. *Polymers* **2018**, *10*, 487.
https://doi.org/10.3390/polym10050487

16. Hu, Y.; Li, Z.; Jiang, L.; Chen, Z.; Liao, L.; Wang, E. *Adv Electron Mater* **2018**, *4*, 1800203.
https://doi.org/10.1002/aelm.201800203

17. Ghosh, S.; Rolland, N.; Zozoulenko, I. *Appl. Phys. Lett.* **2021**, *118*, 223302.
https://doi.org/10.1063/5.0051166

18. Lai, W.C.; Wang, S.H.; Sun, H.S.; Liao, C.W.; Liu, T.Y.; Lee, H.T.; Yang, H.R.; Wang, L.; Lai, Y.Y. *ACS Appl Polym Mater* **2022**, *4*, 521-526.
https://doi.org/10.1021/acsapm.1c01419

19. Song, Y.L.; Ding, J.M.; Dai, X.J.; Li, C.; Di, C.A.; Zhang, D.Q. *ACS Mater Lett* **2022**, *4*, 521-527.
https://doi.org/10.1021/acsmaterialslett.2c00026

20. Wang, S.H.; Chen, P.Z.; Chen, Y.Y.; Khurshid, F.; Cai, C.W.; Lai, Y.Y.; Chung, P.W.; Jeng, R.J.; Rwei, S.P.; Wang, L. *ACS Appl Mater Interfaces* **2022**, *14*, 43109-43115.
https://doi.org/10.1021/acsami.2c08531

21. Wang, S.H.; Fazzi, D.; Puttisong, Y.; Jafari, M.J.; Chen, Z.H.; Ederth, T.; Andreasen, J.W.; Chen, W.M.M.; Facchetti, A.; Fabiano, S. *Chem. Mater.* **2019**, *31*, 3395-3406.
https://doi.org/10.1021/acs.chemmater.9b00558

22. Yang, H.R.; Chen, Y.Y.; Sun, H.S.; Tung, S.H.; Huang, S.L.; Huang, P.C.; Lee, J.J.; Lai, Y.Y. *Macromolecules* **2021**, *54*, 7282-7290.
https://doi.org/10.1021/acs.macromol.1c00308

23. Yang, H.R.; Lai, Y.Y. *Adv Electron Mater* **2021**, *7*, 2000939.
https://doi.org/https://doi.org/10.1002/aelm.202000939

24. Yang, H.R.; Lai, Y.Y.; Lee, J.J. *Adv Electron Mater* **2019**, *5*, 1900213.
https://doi.org/https://doi.org/10.1002/aelm.201900213

25. Yang, H.R.; Pai, C.W.; Sun, H.S.; Wu, C.; Lai, Y.Y.; Haw, S.C.; Lee, J.J.; Chen, J.M. *Macromolecules* **2020**, *53*, 10349-10356.
https://doi.org/10.1021/acs.macromol.0c01559

26. Zhang, G.B.; Yu, H.; Sun, Y.; Wang, W.W.; Zhao, Y.; Wang, L.C.; Qiu, L.Z.; Ding, Y.S. *J. Mater. Chem. C .* **2021**, *9*, 633-639.
https://doi.org/10.1039/d0tc04493h

27. Chang, H.H.; Tsai, C.E.; Lai, Y.Y.; Chiou, D.Y.; Hsu, S.L.; Hsu, C.S.; Cheng, Y.J. *Macromolecules* **2012**, *45*, 9282-9291.
https://doi.org/10.1021/ma3019552

28. Lung.Chen, Y.; Chang, C.Y.; Cheng, Y.J.; Hsu, C.S. *Chem. Mater.* **2012**, *24*, 3964-3971.
https://doi.org/10.1021/cm3024082

29. Cheng, Y.J.; Luh, T.Y. *Macromolecules* **2005**, *38*, 4563-4568.
https://doi.org/10.1021/ma050140z

30. Cheng, Y.J.; Wu, J.S.; Shih, P.I.; Chang, C.Y.; Jwo, P.C.; Kao, W.S.; Hsu, C.S. *Chem. Mater.* **2011**, *23*, 2361-2369.
https://doi.org/10.1021/cm200041v

31. Ito, H.; Segawa, Y.; Murakami, K.; Itami, K. *J. Am. Chem. Soc.* **2019**, *141*, 3-10.
https://doi.org/10.1021/jacs.8b09232

32. Jwo, P.C.; Lai, Y.Y.; Tsai, C.E.; Lai, Y.Y.; Liang, W.W.; Hsu, C.S.; Cheng, Y.J. *Macromolecules* **2014**, *47*, 7386-7396.
https://doi.org/10.1021/ma5018499

33. Luh, T.Y.; Cheng, Y.J. *Chem. Commun.* **2006**, 4669-4678.
https://doi.org/10.1039/B609412K

34. Tseng, C.A.; Wu, J.S.; Lin, T.Y.; Kao, W.S.; Wu, C.E.; Hsu, S.L.; Liao, Y.Y.; Hsu, C.S.; Huang, H.Y.; Hsieh, Y.Z.; Cheng, Y.J. *Chem Asian J.* **2012**, *7*, 2102-2110.
https://doi.org/https://doi.org/10.1002/asia.201200186

35. Wu, J.S.; Cheng, S.W.; Cheng, Y.J.; Hsu, C.S. *Chem. Soc. Rev.* **2015**, *44*, 1113-1154.
https://doi.org/10.1039/C4CS00250D

36. Wu, J.S.; Cheng, Y.J.; Lin, T.Y.; Chang, C.Y.; Shih, P.I.; Hsu, C.S. *Adv. Funct. Mater.* **2012**, *22*, 1711-1722.
https://doi.org/https://doi.org/10.1002/adfm.201102906

37. Zhou, X.H.; Luo, J.; Huang, S.; Kim, T.D.; Shi, Z.; Cheng, Y.J.; Jang, S.H.; Knorr Jr, D.B.; Overney, R.M.; Jen, A.K.Y. *Adv. Mater.* **2009**, *21*, 1976-1981.
https://doi.org/https://doi.org/10.1002/adma.200801639

38. Fukutomi, Y.; Nakano, M.; Hu, J.Y.; Osaka, I.; Takimiya, K. *J. Am. Chem. Soc.* **2013**, *135*, 11445-11448.
https://doi.org/10.1021/ja404753r

39. Nakano, M.; Takimiya, K. *Chem. Mater.* **2017**, *29*, 256-264.
https://doi.org/10.1021/acs.chemmater.6b03413

40. Huang, J.; Chen, Z.; Yang, J.; Ju, H.; Zhang, W.; Yu, G. *Chem. Mater.* **2019**, *31*, 2507-2515.
https://doi.org/10.1021/acs.chemmater.8b05353

41. Chen, Y.; Wang, M.; Zhang, D.; Wang, H.; Deng, W.; Shi, J.; Jie, J. *Appl. Phys. Lett.* **2021**, *119*, 183301.
https://doi.org/10.1063/5.0065403

42. Fregoso, G.; Rupasinghe, G.S.; Shahi, M.; Thorley, K.; Parkin, S.; Paterson, A.F.; Anthony, J. *J. Mater. Chem. C* . **2022**, *10*, 14439-14443.
https://doi.org/10.1039/d2tc02977d

43. Hwang, M.C.; Jang, J.W.; An, T.K.; Park, C.E.; Kim, Y.H.; Kwon, S.K. *Macromolecules* **2012**, *45*, 4520-4528.
https://doi.org/10.1021/ma300540f

44. Jagoo, Z.; Lamport, Z.A.; Jurchescu, O.D.; McNeil, L. *Appl. Phys. Lett.* **2021**, *119*, 073302.
https://doi.org/10.1063/5.0047570

45. Kim, C.H. *Solid State Electron* **2019**, *153*, 23-26.
https://doi.org/10.1016/j.sse.2018.12.014

46. Nakano, M.; Osaka, I.; Hashizume, D.; Takimiya, K. *Chem. Mater.* **2015**, *27*, 6418-6425.
https://doi.org/10.1021/acs.chemmater.5b02601

47. Nasrallah, I.; Ravva, M.K.; Broch, K.; Novak, J.; Armitage, J.; Schweicher, G.; Sadhanala, A.; Anthony, J.E.; Bredas, J.L.; Sirringhaus, H. *Adv Electron Mater* **2020**, *6*, 2000250.
https://doi.org/10.1002/aelm.202000250

48. Tsai, C.-L.; Chan, T.-H.; Lu, H.-C.; Huang, C.-L.; Hung, K.-E.; Lai, Y.-Y.; Cheng, Y.-J. *J. Mater. Chem. A* **2023**, *11*, 7572-7583.
https://doi.org/10.1039/D3TA00519D

49. Lu, T.; Chen, F. *J. Comput. Chem.* **2012**, *33*, 580-592.
https://doi.org/https://doi.org/10.1002/jcc.22885